Elevated ALKBH5 is associated with ferroptosis-related dysfunctions in cytotrophoblasts through FTL in patients with recurrent miscarriage (#94008)

First submission

Guidance from your Editor

Please submit by **14 Feb 2024** for the benefit of the authors (and your token reward) .

Structure and Criteria
Please read the 'Structure and Criteria' page for general guidance.

Custom checks
Make sure you include the custom checks shown below, in your review.

Raw data check
Review the raw data.

Image check
Check that figures and images have not been inappropriately manipulated.

If this article is published your review will be made public. You can choose whether to sign your review. If uploading a PDF please remove any identifiable information (if you want to remain anonymous).

Files

Download and review all files from the materials page.

8 Figure file(s)
1 Table file(s)
2 Other file(s)

Custom checks

Human participant/human tissue checks

- Have you checked the authors ethical approval statement?
- Does the study meet our article requirements?
- Has identifiable info been removed from all files?
- Were the experiments necessary and ethical?

Cell line checks

- Is the correct provenance of the cell line described?

Structure your review

The review form is divided into 5 sections. Please consider these when composing your review:

1. **BASIC REPORTING**
2. **EXPERIMENTAL DESIGN**
3. **VALIDITY OF THE FINDINGS**
4. General comments
5. Confidential notes to the editor

You can also annotate this PDF and upload it as part of your review

When ready submit online.

Editorial Criteria

Use these criteria points to structure your review. The full detailed editorial criteria is on your guidance page.

BASIC REPORTING

- Clear, unambiguous, professional English language used throughout.
- Intro & background to show context. Literature well referenced & relevant.
- Structure conforms to PeerJ standards, discipline norm, or improved for clarity.
- Figures are relevant, high quality, well labelled & described.
- Raw data supplied (see PeerJ policy).

EXPERIMENTAL DESIGN

- Original primary research within Scope of the journal.
- Research question well defined, relevant & meaningful. It is stated how the research fills an identified knowledge gap.
- Rigorous investigation performed to a high technical & ethical standard.
- Methods described with sufficient detail & information to replicate.

VALIDITY OF THE FINDINGS

- Impact and novelty not assessed. *Meaningful* replication encouraged where rationale & benefit to literature is clearly stated.
- All underlying data have been provided; they are robust, statistically sound, & controlled.
- Conclusions are well stated, linked to original research question & limited to supporting results.

Standout reviewing tips

The best reviewers use these techniques

Tip	*Example*
Support criticisms with evidence from the text or from other sources	*Smith et al (J of Methodology, 2005, V3, pp 123) have shown that the analysis you use in Lines 241-250 is not the most appropriate for this situation. Please explain why you used this method.*
Give specific suggestions on how to improve the manuscript	*Your introduction needs more detail. I suggest that you improve the description at lines 57- 86 to provide more justification for your study (specifically, you should expand upon the knowledge gap being filled).*
Comment on language and grammar issues	*The English language should be improved to ensure that an international audience can clearly understand your text. Some examples where the language could be improved include lines 23, 77, 121, 128 – the current phrasing makes comprehension difficult. I suggest you have a colleague who is proficient in English and familiar with the subject matter review your manuscript, or contact a professional editing service.*
Organize by importance of the issues, and number your points	*1. Your most important issue* *2. The next most important item* *3. …* *4. The least important points*
Please provide constructive criticism, and avoid personal opinions	*I thank you for providing the raw data, however your supplemental files need more descriptive metadata identifiers to be useful to future readers. Although your results are compelling, the data analysis should be improved in the following ways: AA, BB, CC*
Comment on strengths (as well as weaknesses) of the manuscript	*I commend the authors for their extensive data set, compiled over many years of detailed fieldwork. In addition, the manuscript is clearly written in professional, unambiguous language. If there is a weakness, it is in the statistical analysis (as I have noted above) which should be improved upon before Acceptance.*

Elevated ALKBH5 is associated with ferroptosis-related dysfunctions in cytotrophoblasts through FTL in patients with recurrent miscarriage

Chuanmei Qin [Equal first author, 1, 2, 3], **Jiayi Wu** [Equal first author, 1, 2, 3], **Xiaowei Wei** [4], **Xueqing Liu** [1, 2, 3], **Yi Lin** [Corresp. 4]

[1] School of Medicine, Shanghai Jiao Tong University, The International Peace Maternity and Child Health Hospital, Shanghai, Shanghai, China

[2] Shanghai Key Laboratory of Embryo Original Diseases, Shanghai, Shanghai, China

[3] School of Medicine, Shanghai Jiao Tong University, Institute of Birth Defects and Rare Diseases, Shanghai, Shanghai, China

[4] School of Medicine, Shanghai Jiao Tong University, Shanghai Jiao Tong University School of Medicine Affiliated Sixth People's Hospital, Shanghai, Shanghai, China

Corresponding Author: Yi Lin
Email address: yilinonline@sjtu.edu.cn

Background: As one of the most common and abundant internal modification in eukaryotic mRNA, N^6-methyladenosine (m^6A) modifications are closely related to placental development. Ferroptosis is a new form of programmed cell death. During placental development, placental trophoblast is susceptible to ferroptosis. Their interactions in trophoblast physiology and injury are unclear. **Methods:** Recurrent miscarriage (RM) was selected as the main gestational disease for our study. The published data (GSE76862) were used to analyze the gene expression profiles in patients with RM. Compared with the quantification of m^6A in total RNA of villous tissues from patients with RM and healthy controls (HC). ALKBH5 was selected as the candidate gene for further research. qRT-PCR, western blotting and immunohistochemistry (IHC) confirmed the elevated expression of ALKBH5 in the cytotrophoblasts of patients with RM. Then, cell counting kit-8 (CCK8) assay, glutathione disulphide/glutathione (GSSG/GSH) quantification, 2′,7′-dichlorfluorescein-diacetate (DCFH-DA) staining and malonaldehyde (MDA) assay was used to explore the alterations of ferroptosis-related characteristics following RAS-selective lethal (RSL3) stimulation after overexpression of ALKBH5. After this, we re-analyzed the published RNA sequencing data upon knockdown of ALKBH5, combined with the tissue RNA-seq data, ferritin light chain (FTL) was identified as the ferroptosis-related gene in cytotrophoblast of patients with RM regulated by ALKBH5. Finally, western blotting and IHC confirmed the increased expression of FTL in the cytotrophoblasts from patients with RM. **Results:** Results showed total m^6A levels were decreased in patients with RM. The most significant differentially m^6A-related gene was ALKBH5, which was increased in patients with RM. In

English

vitro cell experiments showed that treatment with RSL3 resulted in increased cell death and upregulated ALKBH5. Overexpressed ALKBH5 alleviated RSL3-induced HTR8 cell death and caused decreased intracellular oxidation products. Published transcriptome sequencing revealed that FTL was the major ferroptosis-related gene regulated by ALKBH5 in the villous tissues of patients with RM. Consistent with the expression of ALKBH5, FTL was increased by RSL3-induction and increased in patients with RM. **Conclusion:** Elevated ALKBH5 alleviated RSL3-induced cytotrophoblast cell death through promoting the expression of FTL in patients with recurrent miscarriage. Our results supported that ALKBH5 was an important regulator of ferroptosis-related etiology of RM and suggested that ALKBH5 could be responsible for epigenetic aberrations in RM pathogenesis.

? in past tense

Elevated ALKBH5 is associated with ferroptosis-related dysfunctions in cytotrophoblasts through FTL in patients with recurrent miscarriage

Rephrase the title - to minimise shortform

Chuanmei Qin [1, 2,3*], Jiayi Wu [1, 2,3*], Xiaowei Wei [4], Xueqing Liu [1, 2, 3], Yi Lin [4#]

[1]The International Peace Maternity and Child Health Hospital, School of Medicine, Shanghai Jiao Tong University, Shanghai 200030, China;

[2]Shanghai Key Laboratory of Embryo Original Diseases, Shanghai 200030, China;

[3]Institute of Birth Defects and Rare Diseases, School of Medicine, Shanghai Jiao Tong University, Shanghai 200030, China.

[4]Shanghai Jiao Tong University School of Medicine Affiliated Sixth People's Hospital, School of Medicine, Shanghai Jiao Tong University, Shanghai 200233, China;

[*]Chuanmei Qin and Jiayi Wu contributed equally to this work and should be considered as first authors.

Corresponding Author:

Yi Lin

Shanghai Jiao Tong University School of Medicine Affiliated Sixth People's Hospital, Shanghai 200233, China.

Email address: yilinonline@ sjtu.edu.cn

22

Abstract

Background: As one of the most common and abundant internal modification in eukaryotic mRNA, N^6-methyladenosine (m^6A) modifications are closely related to placental development. Ferroptosis is a new form of programmed cell death. During placental development, placental trophoblast is susceptible to ferroptosis. Their interactions in trophoblast physiology and injury are unclear.

Methods: Recurrent miscarriage (RM) was selected as the main gestational disease for our study. The published data (GSE76862) were used to analyze the gene expression profiles in patients with RM. Compared with the quantification of m^6A in total RNA of villous tissues from patients with RM and healthy controls (HC). ALKBH5 was selected as the candidate gene for further research. qRT-PCR, western blotting and immunohistochemistry (IHC) confirmed the elevated expression of ALKBH5 in the cytotrophoblasts of patients with RM. Then, cell counting kit-8 (CCK8) assay, glutathione disulphide/glutathione (GSSG/GSH) quantification, 2′,7′-dichlorfluorescein-diacetate (DCFH-DA) staining and malonaldehyde (MDA) assay was used to explore the alterations of ferroptosis-related characteristics following RAS-selective lethal (RSL3) stimulation after overexpression of ALKBH5. After this, we re-analyzed the published RNA sequencing data upon knockdown of ALKBH5, combined with the published tissue RNA-seq data, ferritin light chain (FTL) was identified as the ferroptosis-related gene in cytotrophoblasts of patients with RM regulated by ALKBH5. Finally, western blotting and IHC confirmed the increased expression of FTL in the cytotrophoblasts from patients with RM.

Results: Results showed total m^6A levels were decreased in patients with RM. The most significant differentially m^6A-related gene was ALKBH5, which was increased in patients with RM. In vitro cell experiments showed that treatment with RSL3 resulted in increased cell death and upregulated ALKBH5. Overexpressed ALKBH5 alleviated RSL3-induced HTR8 cell death and caused decreased intracellular oxidation products. Published transcriptome sequencing revealed that FTL was the major ferroptosis-related gene regulated by ALKBH5 in the villous tissues of patients with RM. Consistent with the expression of ALKBH5, FTL was increased by RSL3-induction and increased in patients with RM.

Conclusion: Elevated ALKBH5 alleviated RSL3-induced cytotrophoblast cell death through promoting the expression of FTL in patients with recurrent miscarriage. Our results supported that ALKBH5 was an important regulator of ferroptosis-related etiology of RM and suggested that ALKBH5 could be responsible for epigenetic aberrations in RM pathogenesis.

Introduction

First sentence has 2 info ie definition and incidence. Rephrase the sentence.

Recurrent miscarriage (RM), defined as two or more consecutive spontaneous abortions with the same sexual partner after confirmed intrauterine pregnancies and before 20-24 gestational weeks, occurs in approximately 1-2% of all couples trying to conceive (Bender Atik et al. 2023; Dimitriadis et al. 2020; Quenby et al. 2023). The cause of RM is complex including chromosomal errors, uterine malformation and autoimmune dysfunction, but the etiology of 40-50% of cases remains unknown (Daimon et al. 2020; Dimitriadis et al. 2020).

Maintenance of pregnancy is a complex and highly regulated biological process requiring coordination of nutrients and immunity between maternal and fetal. Moreover, the coordination needs a functional placenta. The placenta, mainly consisting of maternal decidua and fetal villi, plays a critical role throughout the process of pregnancy (Centurione et al. 2018). As soon as the implantation of the embryo begins, the developing of placenta is initiated with the generating of trophoblast cells from the trophectoderm of the blastocyst (Turco et al. 2018). Cytotrophoblasts (CTBs), an inner layer of the chorionic villi, can differentiate into extravillous CTBs or fuse to form the external layer of syncytiotrophoblasts (STBs) (Costello & Fisher 2021; Hemberger et al. 2020). Before gestational week 11, the developing of the conceptus relies on uterine secretions, then, a villous placenta-blood interface is effectively functional, the exchange of nutrients, gases, and metabolic waste products mainly relies on contact between the maternal blood and fetal villi (Burton et al. 2002; Erlich et al. 2019; Jones et al. 2015). Placental dysfunction associated with impaired trophoblast function may lead to miscarriage, fetal growth restriction, preeclampsia, and stillbirth (Brosens et al. 2011; Turco et al. 2018).

Epigenetic modifications, including histone modifications, DNA methylation, non-coding RNAs and RNA methylation, play functional roles in maternal-fetal medicine (Hocher & Hocher 2018; Wu et al. 2023). N^6-methyladenosine (m^6A) is the most common RNA epigenetic modification, being reported to modulate the biological process of placenta formation and development (Wu et al. 2023). m^6A modification is a complex and reversible process coregulated by m^6A writers, erasers and readers (Zhao et al. 2017). It has been reported m^6A writer complex mainly consists of methyltransferase-like 3 (METTL3), methyltransferase-like 14 (METTL14), and Wilms tumor 1-

associated protein (WTAP), while m^{6}A demethylase (erasers) include fat mass and obesity-associated (FTO), and alkB homolog 5 (ALKBH5), and m^{6}A readers are mainly composed of YT521-B homology domain protein family (YTHDF) (including YTHDF1-3) (Zhang et al. 2023). It has been reported that m^{6}A dysregulations may lead to gestational diseases, such as recurrent miscarriage, preeclampsia, gestational diabetes mellitus (Li et al. 2019; Taniguchi et al. 2020; Wang et al. 2021). Increased ALKBH5 inhibited trophoblast invasion at the maternal-fetal interface of patients with RM (Li et al. 2019). Under fear stress, m^{6}A modifications have been reported play an important role in placental dysfunction during pregnancy (Wang et al. 2022). Moreover, down-regulation of m^{6}A is involved in gestational diabetes mellitus (GDM) development (Wang et al. 2021).

Ferroptosis is a programmed cell death dependent on iron (Jiang et al. 2021). Early in placental development, trophoblast cells experience physiologic hypoxia, which is intimately linked to ferroptosis, leading to placental dysfunction and reproductive disorders (Beharier et al. 2021; Ng et al. 2019). RAS-selective lethal (RSL3) is one of the most important and universal ferroptosis inducers (Yang & Stockwell 2016). In mice experiments, Fer-1 improved outcomes in CBA/J × DBA/2 mice pregnancy (Lai et al. 2024). This suggests that ferroptosis may cause adverse pregnancy outcomes.

This statement does not give direct suggestion. Elaborate/rephrase

Both m^{6}A modification and ferroptosis can regulate pregnancy outcomes, but the link between m^{6}A, ferroptosis and RM pathogenesis is poorly defined. The present study focused on the functional m^{6}A and ferroptosis related genes in recurrent miscarriage, including transcriptomic analysis and identifying the mechanisms affecting the function of trophoblast.

study objective

Materials & Methods

Patient characteristics

15 healthy controls (HC) (mean age, 30.40 ± 2.50 years; mean gestation week, 7.59 ± 0.81 weeks) and 15 patients with RM (mean age, 31.20 ± 4.18 years; mean gestation week, 7.64 ± 1.41 weeks) were recruited from the International Peace Maternity & Child Health Hospital from September 2020 to June 2021. All recruited individuals with HC or RM were under 35 years old and terminated at weeks 6-11 of gestation. Chromosomal abnormalities, endocrine disorders, endometritis, abnormal uterine structure, cervical insufficiency, and other identified etiologies of RM were all excluded. The study was approved by the Medical Ethics Committee of the International Peace Maternity & Child Health Hospital of China Welfare Institute, Shanghai [(GKLW) 2021-49]. Written informed consents were obtained from all the participants (HC, RM).

Please provide sample size calculation

?Terminated by induction

Tissue collection

All villous tissues were collected immediately after induced abortion and cleaned with PBS (Hyclone, Logan, UT, USA) as described before (Wei et al. 2022). For quantitative real-time PCR (qRT-PCR), part of the villous tissues was stored in RNAlater (Thermo Fisher Scientific, Waltham, MA, USA) overnight at 4 °C. Samples were then transferred into liquid nitrogen for long-term storage. For western blotting, part of the villous tissues was snap frozen in liquid nitrogen within 20 min after sampling. For immunohistochemistry, part of the villous tissues was

fixed with 4% paraformaldehyde (PFA) (BBI Life Sciences, Shanghai, China) for 24 h, then embedded in paraffin.

Prussian blue staining

Iron Stain Kit (ab150674, Abcam, Cambridge, UK) was used to determine iron staining in tissue sections. Tissue sections were deparaffinized and rehydrated, then incubated in working iron stain solution for 3min. After rinsed in distilled water, slides were stained in nuclear fast red solution for 5 min and rinsed in 4 changes of distilled water. Slides were dehydrated in 95% alcohol followed by absolute alcohol and mounted. Blue stain shows non chelated iron in the placental villi.

Cell culture

The HTR-8/SVneo cell line was a kind gift from Dr. P.K. Lala (University of Western Ontario, London, ON, Canada) (Graham et al. 1993) and cultured in DMEM/F12 (Gibco, Grand Island, NY, USA) plus 10% fetal bovine serum (Yeasen, Shanghai, China) and 1% penicillin/streptomycin antibiotics (Gibco, Grand Island, NY, USA). Cells were cultured in a 37°C cell culture incubator under atmosphere with 5% CO2.

Transfection protocol

Non-targeting control siRNA (siNC) and ALKBH5 siRNA (siALKBH5) were purchased form GenePharma (Shanghai, China). Oligofectamine ® 2000 Reagent (Invitrogen, Carlsbad, USA) was

146 used for the transfection of siRNA according to the manufacturer's instructions. For
147 overexpression, the pLV-hALKBH5 plasmid and the corresponding pLV empty control plasmid
148 (Vector) were purchased from Cyagen company (Suzhou, China). Transient transfection was
149 performed by the JetPRIME® transfection reagent (Polyplus transfection™, NY, USA). Using a
150 6-well plate as an example, 2 μg of plasmid was added in 200 μl jetPRIME® buffer, followed by
151 addition of 4 μl of jetPRIME® reagent, mixed and incubated 10 min at room temperature. Then
152 the mixture was added to 2ml of serum containing medium in 6-well plate. Cells were transfected
153 at 30-40% confluence. RNA and protein were collected 48 h after transfection. Experiments were
154 repeated three times.
155

156 **RNA isolation and qRT-PCR**

157 The villous tissues or cells were lysed with Trizol (Life Technologies, Carlsbad, CA, USA) and
158 total RNA was extracted according to the reported method (Rio et al. 2010). RNA (1 μg) was
159 reverse transcribed using Evo M-MLV RT Master Mix (Accurate Biology, Hangzhou, China).
160 Quantitative real-time PCR was performed using the SYBR Green Premix Pro Taq HS qPCR Kit
161 (Accurate Biology, China) with the primers listed in **Supplemental Table 1**. Relative mRNA
162 expression normalized to *β-actin* expression was calculated using the $2^{-\Delta\Delta Ct}$ method in cells while
163 the $2^{-\Delta Ct}$ method was used in human tissue samples (Livak & Schmittgen 2001; Schmittgen &
164 Livak 2008). More details are available in the supplemental data: MIQE checklist.
165

166 **Western blotting**

Tissues and cells were lysed in radioimmunoprecipitation assay buffer (Thermo Fisher Scientific, Waltham, USA) containing protease inhibitor cocktail (Solarbio, Beijing, China). Protein concentration was measured using a BCA Protein Assay (Thermo Fisher Scientific). Then, protein was denatured by heating at 100°C for 10 minutes. 10 μg of protein was loaded per well and separated by SDS–PAGE. After electrophoresis, proteins were transferred onto 0.2-μm PVDF membranes (Millipore, Milford, USA), then, blocked with 5% non-fat skim milk at room temperature for 1 h and later incubated with primary antibodies at 4 °C overnight. The following day, the membranes were incubated with secondary antibodies conjugated with HRP for 1 hour at room temperature. The antibodies and dilutions used are as follows: ALKBH5 (1:1000, ab195377, Abcam, Cambridge, UK), FTL (1:1000, ab75973, Abcam, Cambridge, UK), β-Actin (1:10000, 66009-1-Ig, Proteintech, Rosemont, USA), Goat Anti-Rabbit IgG antibody (1:5000, ab288151, Abcam, Cambridge, UK), Goat Anti-Mouse IgG antibody (1:5000, ab7063, Abcam, Cambridge, UK). Signals were detected using the Chemiluminescent HRP Substrate (Millipore) and analyzed using Image J software (NIH, Bethesda, MD, USA). Uncropped western blotting pictures can be found in **Supplemental Figure 1**.

Quantification of m^6A in total RNA

Total RNA methylation was quantified using the EpiQuik M^6A RNA Methylation Quantification Kit (Epigentek, Farmingdale, USA). Total RNA was extracted using Trizol (Life Technologies), then diluted to 200 ng/μl final concentration. The amount of RNA used ~~for~~ per sample was 200ng. RNA sample was transferred to corresponding wells in a Binding Solution-treated 96-well plate.

Each sample were performed in two technical replicates. After binding of RNA, the 96-well plate was incubated with capture antibody at room temperature for 1 h, then washed four times. ? Successively, detection antibody was added into the plate and incubated for 30 min. After washed with washing buffer for five times, the plate was incubated with developer solution about 5 min. Stop solution was added to stop enzyme reaction after color turning blue. Plate was then read for absorbance at 450nm. ?formula for calculation Relative m^6A RNA methylation status was calculated according to the absorbance.

Immunohistochemistry (IHC) assay

Why 10 instead of 15?

Villous tissues from 10 patients with RM and 10 HC controls were washed with PBS immediately after collecting, then, fixed in 4% paraformaldehyde. 48 h later, tissues were paraffin-embedded and serially sectioned. The Mouse and Rabbit specific HRP/diaminobenzidine (DAB) (ABC) Detection IHC Kit (ab64264, Abcam, USA) was used for IHC. The assay was performed according to the manufacturer's instructions. After dewaxing and rehydration, slices were incubated with primary antibody against ALKBH5 (1:1000, ab195377, Abcam, Cambridge, UK) (Wang et al. 2023), FTL (1:500, ab69090, Abcam, Cambridge, UK) (Raha et al. 2022) or Rabbit IgG (1:500, #3900, Cell Signaling Technology) (Tong et al. 2023) diluted in primary antibody dilution (P0277, Beyotime, China). Negative controls were performed during pre-experiments. The following day, slides were incubated with the biotinylated secondary antibody, stained with diaminobenzidine (DAB), counterstained with hematoxylin. After dehydration and mounting, slides were observed

and photographed using microscope. Scoring of slides was independently performed blinded by two pathologists according to the published literature (Liu et al. 2020; Zhao et al. 2019).

Immunofluorescent staining

For immunofluorescence, HTR8 cells were seeded in 24-well plates 1 day before the experiment. The next day, at a confluence of 40%, RSL3 was added at different concentrations (0 μM, 2.5 μM, 5 μM) into plates. 24 h later, the cells were then fixed with 4% paraformaldehyde for 15 min at room temperature, then, blocked and permeabilized with immunol staining blocking buffer (P0102, Beyotime, China) for 20 min at room temperature and subsequently incubated with primary antibodies against ALKBH5 (1:500, 16837-1-AP, Proteintech, Rosemont, USA) overnight at 4 °C (Liu et al. 2021). Next day, the cells were incubated with Alex Fluor 488-conjugated goat anti-Rabbit IgG (Life Technologies, Carlsbad, CA, USA). After washing with PBS for three times, cells were mounted with mounting medium with 4,6-diamino-2-phenylindole (DAPI) (ab104139, Abcam) and observed under a fluorescence microscope (Leica DMi8 microscope, Leica Microsystems, Wetzlar, Germany).

how do you choose the concentraction?

Cell Counting Kit-8 (CCK8) assay

About 2500 cells/per well were plated in 96-well plates 1-day before drug treatment. 1 h before drug treatment, corresponding volumes of DMSO (D2438, Sigma, St. Louis, MO, USA), Ferrostatin-1 (Fer-1, 1 μM, S7243, Selleck, USA), UAMC-3203 (2 μM, S8792, Selleck, USA), necrosulfonamide (1 μM, S8251, Selleck, USA), Z-VAD-FMK (10 μM, S7023, Selleck, USA),

Hydroxychloroquine (HCQ) Sulfate (1 μM, S4430, Selleck, USA) was added to cell culture 2 h before RSL3 (0, 1, 2, 3, 4, 5, 6, 7, 8 μM) was added to cell culture, respectively. Then, 24 h later, the optical density at 450 nm (OD450) was assessed using the Cell Counting Kit-8 (Yeasen, Shanghai, China).

To clarify the role of ALKBH5 in RSL3-induced cell death. About 2000 cells/per well were plated in 96-well plates 1 day prior to transfection of plasmids. Cells at ~30% confluence were transfected with plasmids. 1 day after transfection, cells were treated with RSL3 (5 μM) (Selleck Chemicals, Munich, Germany) or equal volumes of solvent (DMSO) with three duplicate wells in each group. After 24 h, OD450 was assessed.

Glutathione disulphide/glutathione (GSSG/GSH) quantification

GSSG/GSH analysis was performed by the GSSG/GSH Quantification kit (G263, Dojindo, Japan) according to the manufacturer's instructions. 1×10^7 HTR8 cells were collected and washed with PBS, then, lysed twice by freezing and thawing with 80 μl 10 mM HCl. After lysis, 20 μl 5% sulfosalicylic acid (SSA) was added to cell lysate. The supernatant was collected by centrifugation and formulated in ddH_2O to a final concentration of 0.5% SSA. Then, 40 μl GSSG standard solution, GSH standard solution, GSSG sample solution and GSH sample solution were added to 96-well plates respectively. Next, 60 μl buffer solution was added to the plates and incubated at 37 °C for 1 h. After incubating, 60 μl substrate working solution, 60 μl enzyme/coenzyme working solution were added successively. The plates were then moved to a 37 °C incubator for 10 min and the absorbance was measured at 405nm.

250

251 **2′,7′-dichlorfluorescein-diacetate (DCFH-DA) staining**

252 ROS assay kit (R252, Dojindo, Japan) was used for the detection of reactive oxygen species (ROS).
253 HTR8 Cells were plated in six-well plates 1 day before transfection. Next day, the pLV empty and
254 pLV-hALKBH5 plasmid were transfected into cells. 24 h later, about 3500 cells/per well were
255 plated in 96-well plates respectively. The following day, HTR8 cells were washed twice with the
256 hank's balanced salt solution (HBSS). Then, working solution was added into the plate and the
257 plate was incubated at 37 °C with 5% CO_2 for 30 min. After incubation, cells were washed twice
258 with HBSS. Corresponding volumes of DMSO and 5 μM RSL3 were added to cell medium
259 respectively and the plate was then incubated in the incubator for 2 h. Finally, cells were washed
260 twice with HBSS and photographed under the fluorescence microscope immediately.

261

262 **Malonaldehyde (MDA) assay**

263 MDA assay was performed using the lipid peroxidation MDA Assay Kit (S0131S, Beyotime,
264 China). Overexpression of ALKBH5 HTR8 cells and pLV cells were lysed by cell lysis buffer
265 (P0013, Beyotime, China). Following centrifugation for 10 min at 12, 000 × g, the supernatant was
266 collected and the protein concentration of each sample was determined adjusted to the same
267 concentration with lysis buffer using the BCA Protein Assay (Thermo Fisher Scientific). All above
268 operations were carried out in ice bath or 4 °C. 100 μl of either control, sample, or standard was
269 then added to EP tubes. 200 μl MDA working solution was then added to each tube and tubes were
270 incubated at 100 °C for 15 min. After incubation, tubes were centrifugated and 200 μl supernatant

of each sample to be measured was added into 96-well plate. Then, the absorbance at 532 nm was detected. Finally, MDA content of each sample was calculated according to the standard curve.

?formula for calculation

Data analysis of published RNA-sequencing

Published data (GSE76862) were analyzed using GEO2R. Gene IDs conversion, GO and KEGG analyses were done by the clusterProfiler package.

To understand the transcriptional changes caused by ALKBH5, Published RNA-seq data upon knockdown of ALKBH5 was re-analyzed (Li et al. 2019). Differential expression between the groups were performed using the Limma package. Genes were selected by significance threshold of fold change (siALKBH5/siNC) $\geqslant$1.5 or $\leqslant$0.67 and adjusted $P < 0.05$ (Grunseich et al. 2018). ClusterProfiler software was used for GO terms and KEGG pathways enrichment analysis.

Statistical analysis

All experiments were repeated three times. Results are shown as mean values ± standard deviation. Differences between two groups were compared by Student's t-test or Welch's t-test for data displaying a normal distribution. For data that did not conform to a normal distribution, Mann-Whitney test was used to analyze the statistical difference between two groups. $P < 0.05$ was considered statistically significant. GraphPad Prism software version 9 (GraphPad Inc, La Jolla, CA, USA) was used for statistical calculations and presentation.

Results

Iron accumulation in villous trophoblasts of patients with RM

Should not start with "To" in a sentence.

To investigate whether there is iron overload in placental villi, we performed Prussian blue staining of villous tissue sections from HC and RM groups. Prussian blue staining showed iron accumulated at the inner cytotrophoblast layers, and there were significantly more particles in the RM group compared with that in the HC group (**Figure 1A**). To identify the role of ferroptosis-related genes in the regulation of the function of villous trophoblasts during the occurrence of RM, we performed an intersection analysis with the published data (GSE76862) and the FerrDB database (Zhou & Bao 2020). Results showed the top 10 most significant increased and decreased ferroptosis-related genes in the villi of patients with RM (**Figure 1B**). Then, we performed GO and KEGG analyses with the 20 genes (**Figure 1C**). We also identified the protein–protein interactions with the 20 genes using the String database (**Figure 1D**). These prompted that disordered iron metabolism in villous trophoblasts was associated with the onset of RM.

Increased ALKBH5 in cytotrophoblasts of patients with RM

To detect the role of m^6A in the regulation of the function of placental villi, we examined the global m^6A levels in placental villi of patients with RM and HC. Results showed the global m^6A level was lower in patients with RM compared with that in HC (**Figure 2A**). Then we tested the mRNA levels of the major functional m^6A-related genes of the trophoblast tissues from patients with RM or HC (**Figure 2B**). Considering the decreased global m^6A levels in the villous tissues of patients with RM, we chose the m^6A demethylase ALKBH5 as the target gene for further research. qRT-PCR showed the mRNA levels of ALKBH5 was increased in the villous tissues of

patients with RM compared with that in HC (**Figure 2C**), consistent with the protein expression levels detected by western blotting (**Figure 2D, E**). Immunohistochemical staining showed that ALKBH5-positive cells in the first-trimester villous tissues, primarily within the cytotrophoblasts. Results also showed much stronger expression of ALKBH5 was observed in tissues of patients with RM compared with that of HC (**Figure 2F-H**). Thus, ALKBH5 was increased in cytotrophoblasts of patients with RM.

RSL3 increased ALKBH5 during in vitro cell experiments

Trophoblast cell line HTR8/SVneo was used to mimic cytotrophoblasts to clarify the function of ALKBH5 during in vitro experiments. CCK8 assay showed RSL3 caused cell death could be inhibited by Fer-1 (ferroptosis inhibitor) and UAMC-3203 (ferroptosis inhibitor), but could not be inhibited by necrosulfonamide (necrosis inhibitor), Z-VAD-FMK (apoptosis inhibitor) or HCQ (autophagy inhibitor) (**Figure 3A**). The corresponding HTR8 images also agree well with the results (**Figure 3B**). Quantification of m^6A in total RNA showed m^6A levels were decreased by the induction of RSL3 (**Figure 3C**). Then, qRT-PCR showed ALKBH5 was increased by induction of RSL3 (**Figure 3D**), consistent with western blotting results (**Figure 3E, F**) and Immunofluorescent staining (**Figure 3G**). Taken together, the mode of cell death induced by RSL3 suggested ALKBH5 was upregulated during the process of ferroptosis.

ALKBH5 attenuated the events leading to ferroptosis

Characteristics of ferroptosis including insufficient antioxidant capacity (Chen et al. 2023) and enhanced glutathione disulphide/glutathione (GSSG/GSH) levels (Zhu et al. 2022). Considering the elevated ALKBH5 in the cytotrophoblasts of patients with RM, we established HTR8 cells overexpressing ALKBH5 (**Supplemental Figure 2A-C**). CCK8 assay showed higher cells viability after overexpression of ALKBH5 following RSL3 treatment (**Figure 4A**). Consistent with cells viability, GSSG/GSH ratio decreased after ALKBH5 overexpression (**Figure 4B**). Moreover, ALKBH5 decreased reactive oxygen species (ROS) levels induced by RSL3, as detected by DCFH-DA fluorescent dye (**Figure 4C**). Furthermore, MDA level in cells overexpressed ALKBH5 was significantly decreased compared to that in the control group (**Figure 4D**). Taken together, these results indicate that overexpression of ALKBH5 attenuated the characteristics of ferroptosis.

FTL is a functional target of ALKBH5 in trophoblast

To further elucidate the ferroptosis-related target gene of ALKBH5, we re-analyzed a published RNA-seq data (Li et al. 2019). A total of 3183 genes were identified to be dysregulated caused by knockdown of ALKBH5 (**Figure 5A**). GO and KEGG enrichment analyses of the differential genes showed that after knockdown of ALKBH5, cell proliferation and cell death related genes sets were dysregulated (**Figure 5B**). The intersection of the differential genes after knockdown ALKBH5 and the FerrDB database showed there were 47 ferroptosis-related genes dysregulated after knockdown of ALKBH5 (**Figure 5C**). GO and KEGG enrichment analyses were performed using the 47 genes (**Figure 5D**). STRING database showed the interactions between genes

involved in ferroptosis (**Figure 5E**). Heat maps of gene expression for the genes involved in ferroptosis (**Figure 5F**). Compared with the differential genes in Figure 1B, we chose FTL as the candidate gene for further research and established HTR8 cells with ALKBH5 knockdown (**Supplemental Figure 2D-F**). Western blotting showed knockdown of ALKBH5 decreased the expression of FTL (**Figure 6A, B**). Consistent with the results of the knockdown experiments, overexpression of ALKBH5 also upregulated the expression of FTL (**Figure 6C, D**). Moreover, RSL3 stimulation upregulated the expression of FTL (**Figure 6E, F**).

Increased FTL in cytotrophoblasts of patients with RM

For further verification the role of ALKBH5-FTL axis in the pathogenesis of RM, we examined the FTL expression levels in the villous tissues of patients with RM or HC. Western blotting showed FTL was increased in the villi of patients with RM compared with that in HC (**Figure 6G, H**). Immunohistochemical staining also confirmed the expression of FTL was increased in the cytotrophoblasts of patients with RM (**Figure 6I-K**). Summing up, the ALKBH5-FTL axis increased in the cytotrophoblasts of patients with RM.

Discussion

In this study, we found villous samples from patients with RM have higher amount of ALKBH5 and FTL. In vitro experiments revealed that the ferroptosis of HTR-8 was alleviated by ALKBH5 under the induction of RSL3.We further discussed the potential mechanism of m^6A and ferroptosis

in RM. Deciphering the precise and diverse mechanisms in regulating trophoblast cells ferroptosis will offer new insights into RM therapeutic strategy.

The pathogenesis of recurrent miscarriage (RM) is complex and unclear, hence, the treatment of RM remains difficult, resulting in mental and physical suffering to patients and families (Farren et al. 2021; Murphy et al. 2012). Despite a great many of researchers make efforts to elucidate the pathogenesis of recurrent miscarriage and seek treatment options, currently, there are still no effective treatments for RM (Dimitriadis et al. 2020). Therefore, further study of pathogenesis and pathologies of RM is very necessary. Our study revealed that the iron content in the villous tissue of patients with RM is higher than that of normal individuals with higher ALKBH5 and FTL. Also, ALKBH5 alleviated cell death induced by RSL3 and positively regulated the expression of FTL. Together, the study suggests a potential functional role of ALKBH5 in the onset of RM.

Rephrase

Flow is not smooth. Should relate ALKBH5 with m6A.

m^6A is the most common modification on RNA, involving in the regulation of the splicing, translation, and stability of RNA (Bartosovic et al. 2017). Study have found that m^6A modifications functionally regulate trophoblast cells functions thus participating in the pathogenesis of trophoblast dysfunctions and even RM. Based on the previously published transcriptome data (Tian et al. 2016) and the quantification of m^6A in total RNA of villous tissues from patients with RM compared with that in HC, we chose ALKBH5 for further research. ALKBH5 is a m^6A demethylase, which has been shown to play fundamental roles in the onset and development of reproductive disorders. Higher ALKBH5 levels in the villi of patients with RM inhibit the migration and invasion of extravillous trophoblasts (EVTs) by reverse regulating the stability of CYR61 mRNA (Li et al. 2019). Mice experiments showed inhibition of ALKBH5

This is literature review, not discussion.

Rephrase

alleviated preeclampsia-like symptoms through the Wnt/β-catenin pathway (Guo et al. 2022). In our study, combined the published RNA-seq data of HTR8 cells upon ALKBH5 knockdown, the published RNA-seq data of patients with RM and HC and the FerrDB database, FTL was identified as the candidate gene. FTL and ferritin heavy chain (FTH1) constitute ferritin acting as an iron reservoir responsible for storing and releasing iron (Gatica et al. 2018). Most literatures reported that overexpression of FTL promoted iron storage therefore inhibiting ferroptosis (Chen et al. 2020; Xie et al. 2016). Consistent with the function of alleviating ferroptosis of overexpressed ALKBH5. It has been reported the content of Fe^{2+} in the implantation site of RM mice was higher than that in control group (Lai et al. 2024). Consistent with this model, our results showed enhanced Prussian blue staining in the villous tissues of RM. Collectively, these results suggested that ferroptosis occurred in RM. Then, we detected increased ALKBH5 and FTL in patients with RM and the resistant function to ferroptosis of ALKBH5. Finally, we identified the expression of FTL, a gene regulating the storage of iron, was regulated by ALKBH5. Our results showed that the ALKBH5-FTL axis was upregulated during ferroptosis in cytotrophoblasts, and resistant to ferroptosis. However, ALKBH5 and FTL, the genes of resistance to ferroptosis were elevated in the RM group with ferroptosis aggravated suggesting that the complex biological function of ALKBH5 remains to be explored. Nevertheless, there are still limitations to the study. The mechanism of ALKBH5 regulating the expression of FTL and the function of ALKBH5-FTL axis on the pregnancy outcome are unclear.

Collectively, by comparing the published tissue RNA-seq data, ALKBH5 knockdown HTR8 cells RNA-seq data, and the the FerrDB database, this study provides new insights into the

pathomechanism of RM by exploring the function of ALKBH5. To study whether ALKBH5-FTL has direct effect on pregnancy outcome, MeRIP-seq and in vivo experiments are required. Our study will help to understand the pathogenesis of RM and provide guidance to predict the onset of RM. Furthermore, the ALKBH5-FTL axis may have potential therapeutic value for the treatment of RM.

Conclusions

In conclusion, the study suggested that recurrent miscarriage may result from ferroptosis of cytotrophoblasts. ALKBH5 was increased in the cytotrophoblasts of patients with RM compared with HC. Furthermore, ALKBH5 alleviated the ferroptosis-associated characteristics induced by RSL3. Finally, we confirmed ALKBH5 regulated the expression of FTL in cytotrophoblasts. In summary, elevated ALKBH5 in cytotrophoblasts of patients with RM alleviated ferroptosis through regulation of FTL.

Acknowledgements

We are grateful to Dr. Fu-Ju Tian for his mentorship and guidance.

433 **References**

434 Bartosovic M, Molares H, Gregorova P, Hrossova D, Kudla G, and Vanacova S. 2017. N6-
435 methyladenosine demethylase FTO targets pre-mRNAs and regulates alternative splicing
436 and 3'-end processing. *Nucleic acids research* 45:11356-11370. 10.1093/nar/gkx778
437 Beharier O, Kajiwara K, and Sadovsky Y. 2021. Ferroptosis, trophoblast lipotoxic damage, and
438 adverse pregnancy outcome. *Placenta* 108:32-38. 10.1016/j.placenta.2021.03.007
439 Bender Atik R, Christiansen O, Elson J, Kolte A, Lewis S, Middeldorp S, Mcheik S, Peramo B,
440 Quenby S, Nielsen H, van der Hoorn M, Vermeulen N, and Goddijn M. 2023. ESHRE
441 guideline: recurrent pregnancy loss: an update in 2022. *Human reproduction open*
442 2023:hoad002. 10.1093/hropen/hoad002
443 Brosens I, Pijnenborg R, Vercruysse L, and Romero R. 2011. The "Great Obstetrical Syndromes"
444 are associated with disorders of deep placentation. *American journal of obstetrics and*
445 *gynecology* 204:193-201. 10.1016/j.ajog.2010.08.009
446 Burton G, Watson A, Hempstock J, Skepper J, and Jauniaux E. 2002. Uterine glands provide
447 histiotrophic nutrition for the human fetus during the first trimester of pregnancy. *The*
448 *Journal of clinical endocrinology and metabolism* 87:2954-2959. 10.1210/jcem.87.6.8563
449 Centurione L, Passaretta F, Centurione M, Munari S, Vertua E, Silini A, Liberati M, Parolini O,
450 and Di Pietro R. 2018. Mapping of the Human Placenta: Experimental Evidence of
451 Amniotic Epithelial Cell Heterogeneity. *Cell transplantation* 27:12-22.
452 10.1177/0963689717725078
453 Chen B, Zhao L, Yang R, and Xu T. 2023. The recent advancements of ferroptosis in the diagnosis,

treatment and prognosis of ovarian cancer. *Frontiers in genetics* 14:1275154. 10.3389/fgene.2023.1275154

Chen PH, Wu J, Ding CC, Lin CC, Pan S, Bossa N, Xu Y, Yang WH, Mathey-Prevot B, and Chi JT. 2020. Kinome screen of ferroptosis reveals a novel role of ATM in regulating iron metabolism. *Cell Death Differ* 27:1008-1022. 10.1038/s41418-019-0393-7

Costello J, and Fisher S. 2021. The Placenta - Fast, Loose, and in Control. *The New England journal of medicine* 385:87-89. 10.1056/NEJMcibr2106321

Daimon A, Morihara H, Tomoda K, Morita N, Koishi Y, Kanki K, Ohmichi M, and Asahi M. 2020. Intravenously Injected Pluripotent Stem Cell-derived Cells Form Fetomaternal Vasculature and Prevent Miscarriage in Mouse. *Cell transplantation* 29. Artn 0963689720970456

10.1177/0963689720970456

Dimitriadis E, Menkhorst E, Saito S, Kutteh W, and Brosens J. 2020. Recurrent pregnancy loss. *Nature reviews Disease primers* 6:98. 10.1038/s41572-020-00228-z

Erlich A, Pearce P, Mayo R, Jensen O, and Chernyavsky I. 2019. Physical and geometric determinants of transport in fetoplacental microvascular networks. *Science advances* 5:eaav6326. 10.1126/sciadv.aav6326

Farren J, Jalmbrant M, Falconieri N, Mitchell-Jones N, Bobdiwala S, Al-Memar M, Tapp S, Van Calster B, Wynants L, Timmerman D, and Bourne T. 2021. Differences in post-traumatic stress, anxiety and depression following miscarriage or ectopic pregnancy between women and their partners: multicenter prospective cohort study. *Ultrasound in obstetrics &*

gynecology : the official journal of the International Society of Ultrasound in Obstetrics and Gynecology 57:141-148. 10.1002/uog.23147

Gatica D, Lahiri V, and Klionsky DJ. 2018. Cargo recognition and degradation by selective autophagy. *Nat Cell Biol* 20:233-242. 10.1038/s41556-018-0037-z

Graham CH, Hawley TS, Hawley RG, MacDougall JR, Kerbel RS, Khoo N, and Lala PK. 1993. Establishment and characterization of first trimester human trophoblast cells with extended lifespan. *Exp Cell Res* 206:204-211. 10.1006/excr.1993.1139

Grunseich C, Wang IX, Watts JA, Burdick JT, Guber RD, Zhu Z, Bruzel A, Lanman T, Chen K, Schindler AB, Edwards N, Ray-Chaudhury A, Yao J, Lehky T, Piszczek G, Crain B, Fischbeck KH, and Cheung VG. 2018. Senataxin Mutation Reveals How R-Loops Promote Transcription by Blocking DNA Methylation at Gene Promoters. Mol Cell 69:426-437.e427. 10.1016/j.molcel.2017.12.030

Guo Y, Song W, and Yang Y. 2022. Inhibition of ALKBH5-mediated m A modification of PPARG mRNA alleviates H/R-induced oxidative stress and apoptosis in placenta trophoblast. *Environmental toxicology* 37:910-924. 10.1002/tox.23454

Hemberger M, Hanna C, and Dean W. 2020. Mechanisms of early placental development in mouse and humans. *Nature reviews Genetics* 21:27-43. 10.1038/s41576-019-0169-4

Hocher B, and Hocher C. 2018. Epigenetics of recurrent pregnancy loss. *EBioMedicine* 35:18-19. 10.1016/j.ebiom.2018.08.046

Jiang X, Stockwell B, and Conrad M. 2021. Ferroptosis: mechanisms, biology and role in disease. *Nature reviews Molecular cell biology* 22:266-282. 10.1038/s41580-020-00324-8

Jones C, Choudhury R, and Aplin J. 2015. Tracking nutrient transfer at the human maternofetal interface from 4 weeks to term. *Placenta* 36:372-380. 10.1016/j.placenta.2015.01.002

Lai Y, Zhang Y, Zhang H, Chen Z, Zeng L, Deng G, Luo S, and Gao J. 2024. Modified Shoutai Pill inhibited ferroptosis to alleviate recurrent pregnancy loss. *Journal of ethnopharmacology* 319:117028. 10.1016/j.jep.2023.117028

Li X, Jin F, Wang B, Yin X, Hong W, and Tian F. 2019. CYR61The m6A demethylase ALKBH5 controls trophoblast invasion at the maternal-fetal interface by regulating the stability of mRNA. *Theranostics* 9:3853-3865. 10.7150/thno.31868

Liu J, Xu YP, Li K, Ye Q, Zhou HY, Sun H, Li X, Yu L, Deng YQ, Li RT, Cheng ML, He B, Zhou J, Li XF, Wu A, Yi C, and Qin CF. 2021. The m(6)A methylome of SARS-CoV-2 in host cells. *Cell Res* 31:404-414. 10.1038/s41422-020-00465-7

Liu XY, Jiang W, Ma D, Ge LP, Yang YS, Gou ZC, Xu XE, Shao ZM, and Jiang YZ. 2020. SYTL4 downregulates microtubule stability and confers paclitaxel resistance in triple-negative breast cancer. *Theranostics* 10:10940-10956. 10.7150/thno.45207

Livak K, and Schmittgen T. 2001. Analysis of relative gene expression data using real-time quantitative PCR and the 2(-Delta Delta C(T)) Method. *Methods (San Diego, Calif)* 25:402-408. 10.1006/meth.2001.1262

Murphy F, Lipp A, and Powles D. 2012. Follow-up for improving psychological well being for women after a miscarriage. *The Cochrane database of systematic reviews* 3:CD008679. 10.1002/14651858.CD008679.pub2

Ng S, Norwitz S, and Norwitz E. 2019. The Impact of Iron Overload and Ferroptosis on

Reproductive Disorders in Humans: Implications for Preeclampsia. *International journal of molecular sciences* 20. 10.3390/ijms20133283

Quenby S, Booth K, Hiller L, Coomarasamy A, de Jong P, Hamulyák E, Scheres L, van Haaps T, Ewington L, Tewary S, Goddijn M, and Middeldorp S. 2023. Heparin for women with recurrent miscarriage and inherited thrombophilia (ALIFE2): an international open-label, randomised controlled trial. *Lancet (London, England)* 402:54-61. 10.1016/s0140-6736(23)00693-1

Raha AA, Biswas A, Henderson J, Chakraborty S, Holland A, Friedland RP, Mukaetova-Ladinska E, Zaman S, and Raha-Chowdhury R. 2022. Interplay of Ferritin Accumulation and Ferroportin Loss in Ageing Brain: Implication for Protein Aggregation in Down Syndrome Dementia, Alzheimer's, and Parkinson's Diseases. *Int J Mol Sci* 23. 10.3390/ijms23031060

Rio D, Ares M, Hannon G, and Nilsen T. 2010. Purification of RNA using TRIzol (TRI reagent). *Cold Spring Harbor protocols* 2010:pdb.prot5439. 10.1101/pdb.prot5439

Schmittgen T, and Livak K. 2008. Analyzing real-time PCR data by the comparative C(T) method. *Nature protocols* 3:1101-1108. 10.1038/nprot.2008.73

Taniguchi K, Kawai T, Kitawaki J, Tomikawa J, Nakabayashi K, Okamura K, Sago H, and Hata K. 2020. Epitranscriptomic profiling in human placenta: N6-methyladenosine modification at the 5'-untranslated region is related to fetal growth and preeclampsia. *FASEB journal : official publication of the Federation of American Societies for Experimental Biology* 34:494-512. 10.1096/fj.201900619RR

Tian F, Cheng Y, Li X, Wang F, Qin C, Ma X, Yang J, and Lin Y. 2016. The YY1/MMP2 axis

promotes trophoblast invasion at the maternal-fetal interface. *The Journal of pathology* 239:36-47. 10.1002/path.4694

Tong G, Chen Y, Chen X, Fan J, Zhu K, Hu Z, Li S, Zhu J, Feng J, Wu Z, Hu Z, Zhou B, Jin L, Chen H, Shen J, Cong W, and Li X. 2023. FGF18 alleviates hepatic ischemia-reperfusion injury via the USP16-mediated KEAP1/Nrf2 signaling pathway in male mice. *Nat Commun* 14:6107. 10.1038/s41467-023-41800-x

Turco M, Gardner L, Kay R, Hamilton R, Prater M, Hollinshead M, McWhinnie A, Esposito L, Fernando R, Skelton H, Reimann F, Gribble F, Sharkey A, Marsh S, O'Rahilly S, Hemberger M, Burton G, and Moffett A. 2018. Trophoblast organoids as a model for maternal-fetal interactions during human placentation. *Nature* 564:263-267. 10.1038/s41586-018-0753-3

Wang J, Wang K, Liu W, Cai Y, and Jin H. 2021. m6A mRNA methylation regulates the development of gestational diabetes mellitus in Han Chinese women. *Genomics* 113:1048-1056. 10.1016/j.ygeno.2021.02.016

Wang Q, Pan M, Zhang T, Jiang Y, Zhao P, Liu X, Gao A, Yang L, and Hou J. 2022. Fear Stress During Pregnancy Affects Placental m6A-Modifying Enzyme Expression and Epigenetic Modification Levels. *Front Genet* 13:927615. 10.3389/fgene.2022.927615

Wang W, Huang Q, Liao Z, Zhang H, Liu Y, Liu F, Chen X, Zhang B, Chen Y, and Zhu P. 2023. ALKBH5 prevents hepatocellular carcinoma progression by post-transcriptional inhibition of PAQR4 in an m6A dependent manner. *Exp Hematol Oncol* 12:1. 10.1186/s40164-022-00370-2

Wei XW, Liu XQ, Zhang YC, Qin CM, Lin Y, and Tian FJ. 2022. TCF3 regulates human endometrial stromal cell proliferation and migration in RPL. *Reproduction* 163:281-291. 10.1530/REP-21-0463

Wu S, Liu K, Zhou B, and Wu S. 2023. N6-methyladenosine modifications in maternal-fetal crosstalk and gestational diseases. *Front Cell Dev Biol* 11:1164706. 10.3389/fcell.2023.1164706

Xie Y, Hou W, Song X, Yu Y, Huang J, Sun X, Kang R, and Tang D. 2016. Ferroptosis: process and function. *Cell Death Differ* 23:369-379. 10.1038/cdd.2015.158

Yang W, and Stockwell B. 2016. Ferroptosis: Death by Lipid Peroxidation. *Trends in cell biology* 26:165-176. 10.1016/j.tcb.2015.10.014

Zhang T, Jiang Z, Yang N, Ge Z, Zuo Q, Huang S, and Sun L. 2023. N6-methyladenosine (m6A) Modification in Preeclampsia. *Reproductive Sciences*. 10.1007/s43032-023-01250-8

Zhao B, Roundtree I, and He C. 2017. Post-transcriptional gene regulation by mRNA modifications. *Nature reviews Molecular cell biology* 18:31-42. 10.1038/nrm.2016.132

Zhao S, Liu XY, Jin X, Ma D, Xiao Y, Shao ZM, and Jiang YZ. 2019. Molecular portraits and trastuzumab responsiveness of estrogen receptor-positive, progesterone receptor-positive, and HER2-positive breast cancer. *Theranostics* 9:4935-4945. 10.7150/thno.35730

Zhou N, and Bao J. 2020. FerrDb: a manually curated resource for regulators and markers of ferroptosis and ferroptosis-disease associations. *Database : the journal of biological databases and curation* 2020. 10.1093/database/baaa021

Zhu R, Gao C, Feng Q, Guan H, Wu J, Samant H, Yang F, and Wang X. 2022. Ferroptosis-related

genes with post-transcriptional regulation mechanisms in hepatocellular carcinoma determined by bioinformatics and experimental validation. *Annals of Translational Medicine* 10:1390. 10.21037/atm-22-5750

585 **Figure Legends**

586 **Figure 1. Iron accumulation in villous trophoblasts of patients with RM.** (A) Prussian blue
587 staining on villous tissues from the patients with RM (N= 10) or HC (N = 10). (B) Gene lists from
588 published GSE76862 and the FerrDB database were ranked by fold change. (C) GO and KEGG
589 enrichment analysis performed using genes listed in (B). (D) Network analysis of genes listed in
590 (B) from the String database.

591

592 **Figure 2. ALKBH5 was increased in the villous tissues from patients with RM.** (A) Total m^6A
593 level of each villous tissue from patients with RM (n = 15) or HC (n = 15). (B) Detection of m^6A
594 reader, writer, and eraser mRNA by qRT-PCR. (C) qRT-PCR showing that *ALKBH5* was
595 increased in the villous tissues of patients with RM (n = 15) compared with that in HC (N = 15).
596 (D, E) Western blot showing that ALKBH5 was increased in the villous tissues of patients with
597 RM (n = 14) compared with that in HC (N = 14). (F, G, H) Representative immunohistochemical
598 images depicting the expression of ALKBH5 in the villous tissues from patients with RM (n = 10)
599 and HC (n = 10). (CTB, cytotrophoblast; STB, syncytiotrophoblast; $*p < 0.05$; $**p < 0.01$).

600

601 **Figure 3. RSL3 promoted the expression of ALKBH5.** (A) RSL3-induced HTR8 cell death can
602 be rescued by Ferrostatin-1 (Fer-1) and UAMC-3203, but not necrosulfonamide, Z-VAD-FMK
603 and Hydroxychloroquine (HCQ) Sulfate (HCQ). (B) Representative picture of HTR8 cell
604 morphology after 24 h treatment. (C) Quantification of m^6A in total RNA after RSL3-induced for
605 24 h. (D) qRT-PCR showing *ALKBH5* was increased after RSL3-induced for 24 h. (E, F) Western

blot showing that ALKBH5 was increased after RSL3-induced for 24 h. (G) Immunofluorescent images showing HTR8 cells with ALKBH5 elevated expression after RSL3-induced for 24 h. Experiments were repeated three times. (**$p < 0.01$).

Figure 4. Characteristics of ferroptosis of HTR8 cells after overexpression of ALKBH5. (A) CCK8 showing overexpression of ALKBH5 alleviated RSL3 induced cell death. (B) GSSG/GSH quantification showing overexpression of ALKBH5 alleviated RSL3 induced GSSG/GSH imbalances. (C) DCFH-DA staining showing overexpression of ALKBH5 alleviated RSL3 induced generation of ROS. (D) MDA assay showing overexpression of ALKBH5 alleviated RSL3 induced generation of MDA. Experiments were repeated three times. (*$p < 0.05$; **$p < 0.01$).

Figure 5. The published transcriptomes of knockdown ALKBH5 HTR8 cells and control cells. (A) The volcano plot showing gene expression changes after ALKBH5 knockdown. (B) GO and KEGG enrichment analysis after ALKBH5 knockdown. (C) Venn diagram showing intersection of the differential genes after ALKBH5 knockdown and gene lists from the FerrDB database. (D) GO and KEGG enrichment analysis performed using the 47 genes in (C). (E)Network analysis of Ferroptosis-related genes in (D) from String database. (F) Heat map showing ferroptosis-related genes expression levels.

Figure 6. ALKBH5 regulated the expression of FTL. (A, B) Western blot showing that knockdown ALKBH5 reduced FTL protein levels. Experiments were repeated three times. (C, D)

Western blot showing that overexpression of ALKBH5 increased FTL protein levels. Experiments were repeated three times. (E, F) Western blot showing that RSL3 increased the expression of FTL. Experiments were repeated three times. (G, H) Western blot showing that FTL was increased in the villous tissues of patients with RM (n = 14) compared with that in HC (N = 14). (I, J, K) Representative immunohistochemical images depicting the expression of FTL in the villous tissues from patients with RM (n = 10) and HC (n = 10). (CTB, cytotrophoblast; STB, syncytiotrophoblast; *$p < 0.05$; **$p < 0.01$).

Figure 1

Iron accumulation in villous trophoblasts of patients with RM.

(A) Prussian blue staining on villous tissues from the patients with RM (N= 10) or HC (N = 10). (B) Gene lists from published GSE76862 and the FerrDB database were ranked by fold change. (C) GO and KEGG enrichment analysis performed using genes listed in (B). (D) Network analysis of genes listed in (B) from the String database.

Figure 1

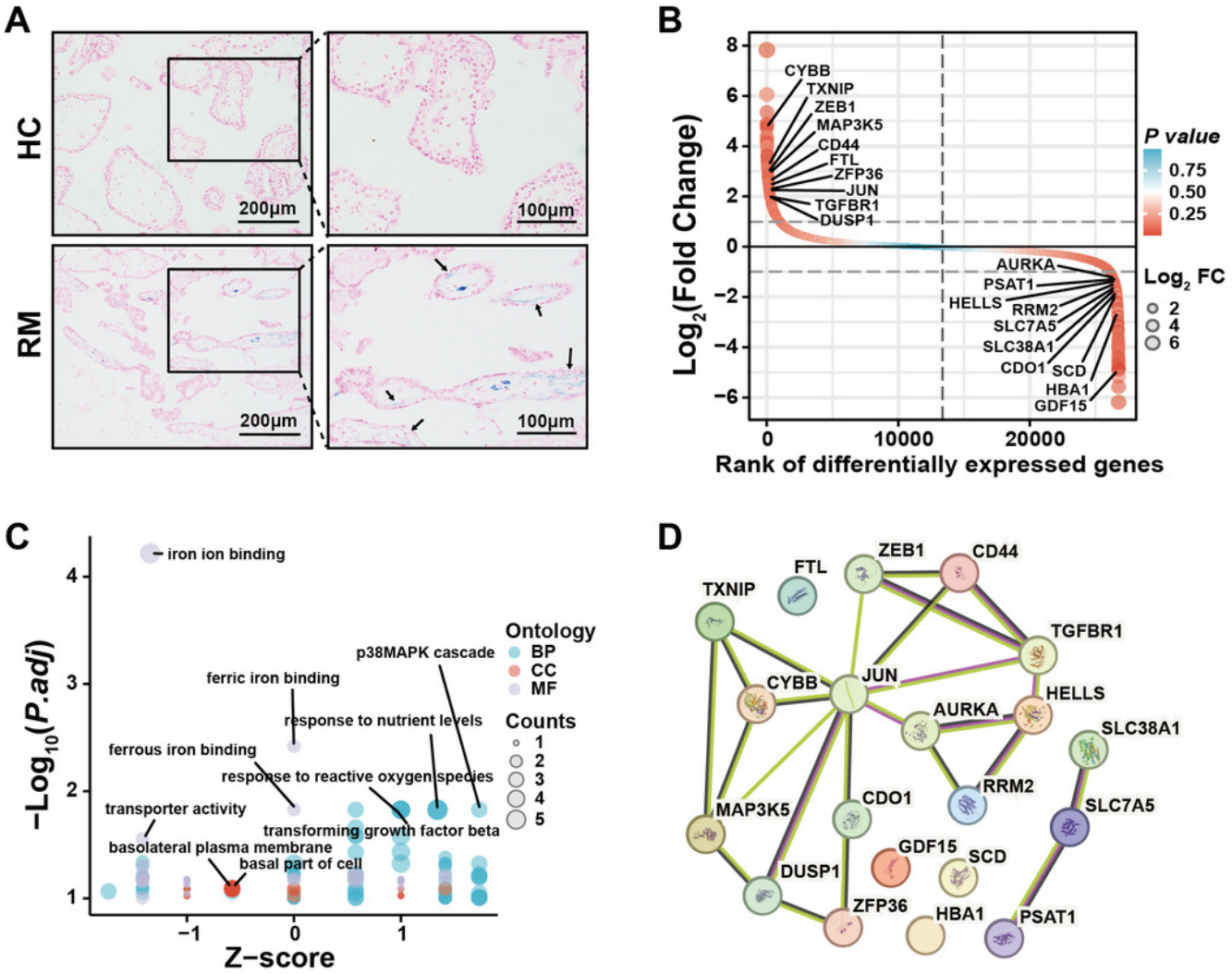
A
HC
RM
200μm
100μm
200μm
100μm
B
CYBB
TXNIP
ZEB1
MAP3K5
CD44
FTL
ZFP36
JUN
TGFBR1
DUSP1
AURKA
PSAT1
HELLS
RRM2
SLC7A5
SLC38A1
CDO1
SCD
HBA1
GDF15
P value
0.75
0.50
0.25
Log2 FC
2
4
6
Log2(Fold Change)
Rank of differentially expressed genes
C
iron ion binding
p38MAPK cascade
ferric iron binding
response to nutrient levels
ferrous iron binding
response to reactive oxygen species
transporter activity
transforming growth factor beta
basolateral plasma membrane
basal part of cell
Ontology
BP
CC
MF
Counts
1
2
3
4
5
−Log10(P.adj)
Z−score
D
TXNIP
FTL
ZEB1
CD44
TGFBR1
CYBB
JUN
HELLS
AURKA
SLC38A1
RRM2
SLC7A5
MAP3K5
CDO1
GDF15
SCD
DUSP1
ZFP36
HBA1
PSAT1

Figure 2

ALKBH5 was increased in the villous tissues from patients with RM.

(A) Total m^6A level of each villous tissue from patients with RM (n = 15) or HC (n = 15). (B) Detection of m^6A reader, writer, and eraser mRNA by qRT-PCR. (C) qRT-PCR showing that *ALKBH5* was increased in the villous tissues of patients with RM (n = 15) compared with that in HC (N = 15). (D, E) Western blot showing that ALKBH5 was increased in the villous tissues of patients with RM (n = 14) compared with that in HC (N = 14). (F, G, H) Representative immunohistochemical images depicting the expression of ALKBH5 in the villous tissues from patients with RM (n = 10) and HC (n = 10). (CTB, cytotrophoblast; STB, syncytiotrophoblast; *$p < 0.05$; **$p < 0.01$).

Figure 2

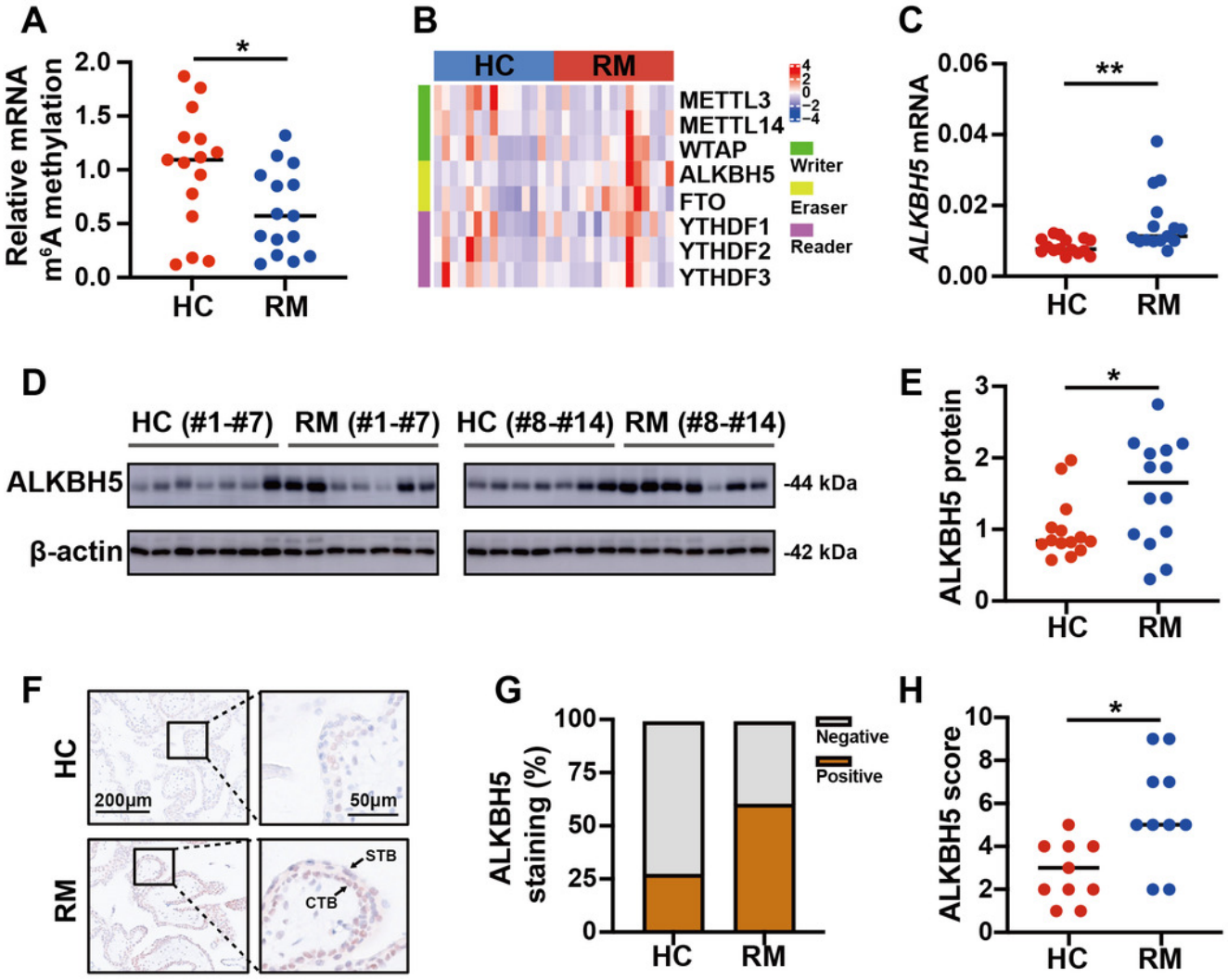
A
Relative mRNA m6A methylation
2.0
1.5
1.0
0.5
0.0
*
HC
RM
B
HC
RM
METTL3
METTL14
WTAP
ALKBH5
FTO
YTHDF1
YTHDF2
YTHDF3
Writer
Eraser
Reader
4
2
0
−2
−4
C
ALKBH5 mRNA
0.06
0.04
0.02
0.00
**
HC
RM
D
HC (#1-#7)
RM (#1-#7)
HC (#8-#14)
RM (#8-#14)
ALKBH5
β-actin
-44 kDa
-42 kDa
E
ALKBH5 protein
3
2
1
0
*
HC
RM
F
HC
RM
200μm
50μm
STB
CTB
G
ALKBH5 staining (%)
100
75
50
25
0
Negative
Positive
HC
RM
H
ALKBH5 score
10
8
6
4
2
0
*
HC
RM

Figure 3

RSL3 promoted the expression of ALKBH5.

(A) RSL3-induced HTR8 cell death can be rescued by Ferrostatin-1 (Fer-1) and UAMC-3203, but not necrosulfonamide, Z-VAD-FMK and Hydroxychloroquine (HCQ) Sulfate (HCQ). (B) Representative picture of HTR8 cell morphology after 24 h treatment. (C) Quantification of m^6A in total RNA after RSL3-induced for 24 h. (D) qRT-PCR showing *ALKBH5* was increased after RSL3-induced for 24 h. (E, F) Western blot showing that ALKBH5 was increased after RSL3-induced for 24 h. (G) Immunofluorescent images showing HTR8 cells with ALKBH5 elevated expression after RSL3-induced for 24 h. (**$p < 0.01$).

Figure 3

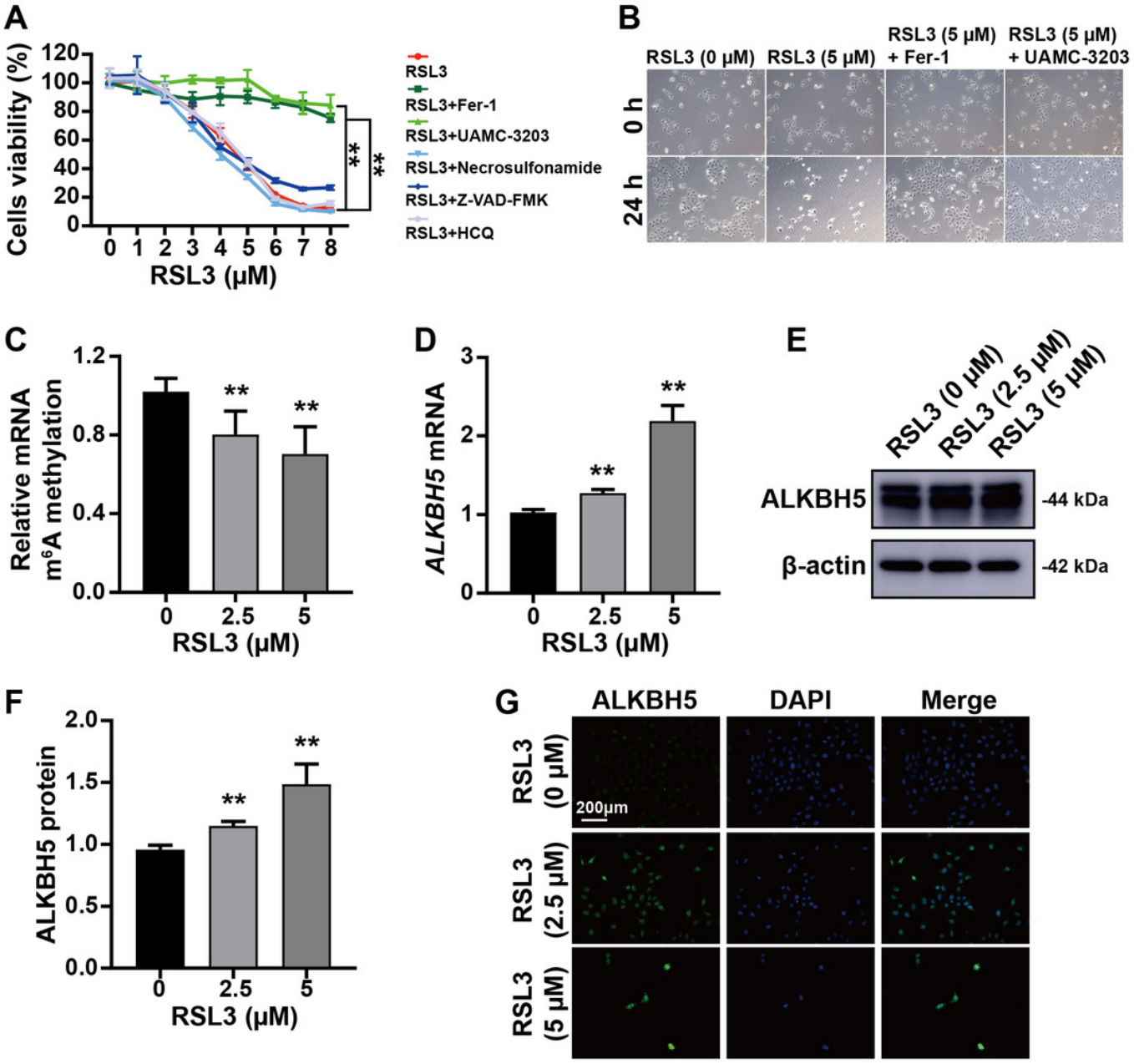
A
Cells viability (%)
RSL3 (μM)
RSL3
RSL3+Fer-1
RSL3+UAMC-3203
RSL3+Necrosulfonamide
RSL3+Z-VAD-FMK
RSL3+HCQ
B
RSL3 (0 μM)
RSL3 (5 μM)
RSL3 (5 μM) + Fer-1
RSL3 (5 μM) + UAMC-3203
0 h
24 h
C
Relative mRNA m6A methylation
RSL3 (μM)
D
ALKBH5 mRNA
RSL3 (μM)
E
RSL3 (0 μM)
RSL3 (2.5 μM)
RSL3 (5 μM)
ALKBH5
-44 kDa
β-actin
-42 kDa
F
ALKBH5 protein
RSL3 (μM)
G
ALKBH5
DAPI
Merge
RSL3 (0 μM)
RSL3 (2.5 μM)
RSL3 (5 μM)
200μm

Figure 4

Characteristics of ferroptosis of HTR8 cells after overexpression of ALKBH5.

(A) CCK8 showing overexpression of ALKBH5 alleviated RSL3 induced cell death. (B) GSSG/GSH quantification showing overexpression of ALKBH5 alleviated RSL3 induced GSSG/GSH imbalances. (C) DCFH-DA staining showing overexpression of ALKBH5 alleviated RSL3 induced generation of ROS. (D) MDA assay showing overexpression of ALKBH5 alleviated RSL3 induced generation of MDA. (*$p < 0.05$; **$p < 0.01$).

Figure 4

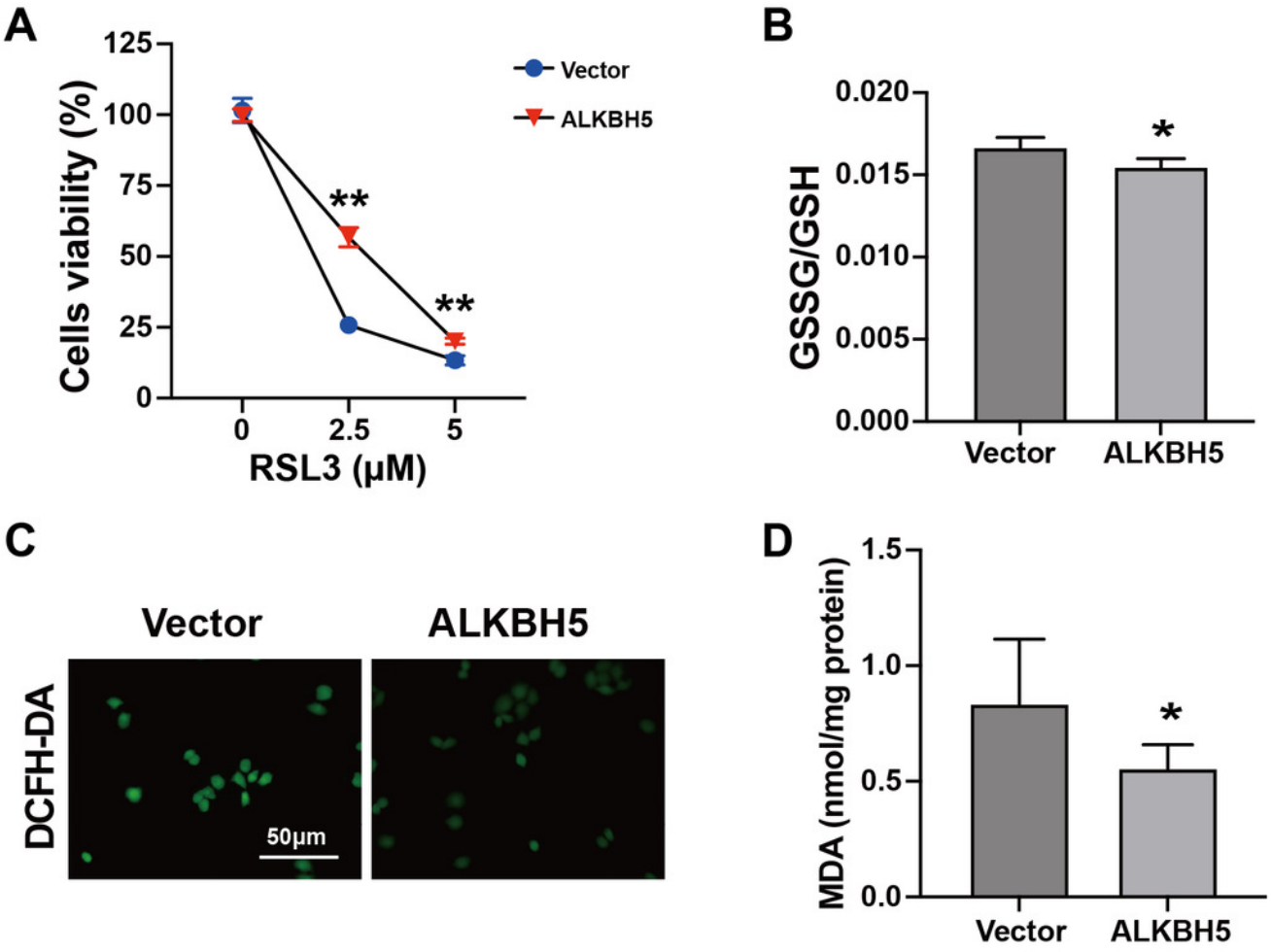
A
Cells viability (%)
125
100
75
50
25
0
0
2.5
5
RSL3 (μM)
Vector
ALKBH5
**
**
B
GSSG/GSH
0.020
0.015
0.010
0.005
0.000
*
Vector
ALKBH5
C
Vector
ALKBH5
DCFH-DA
50μm
D
MDA (nmol/mg protein)
1.5
1.0
0.5
0.0
*
Vector
ALKBH5

Figure 5

The published transcriptomes of knockdown ALKBH5 HTR8 cells and control cells.

(A) The volcano plot showing gene expression changes after ALKBH5 knockdown. (B) GO and KEGG enrichment analysis after ALKBH5 knockdown. (C) Venn diagram showing intersection of the differential genes after ALKBH5 knockdown and gene lists from the FerrDB database. (D) GO and KEGG enrichment analysis performed using the 47 genes in (C). (E)Network analysis of Ferroptosis-related genes in (D) from String database. (F) Heat map showing ferroptosis-related genes expression levels.

Figure 5

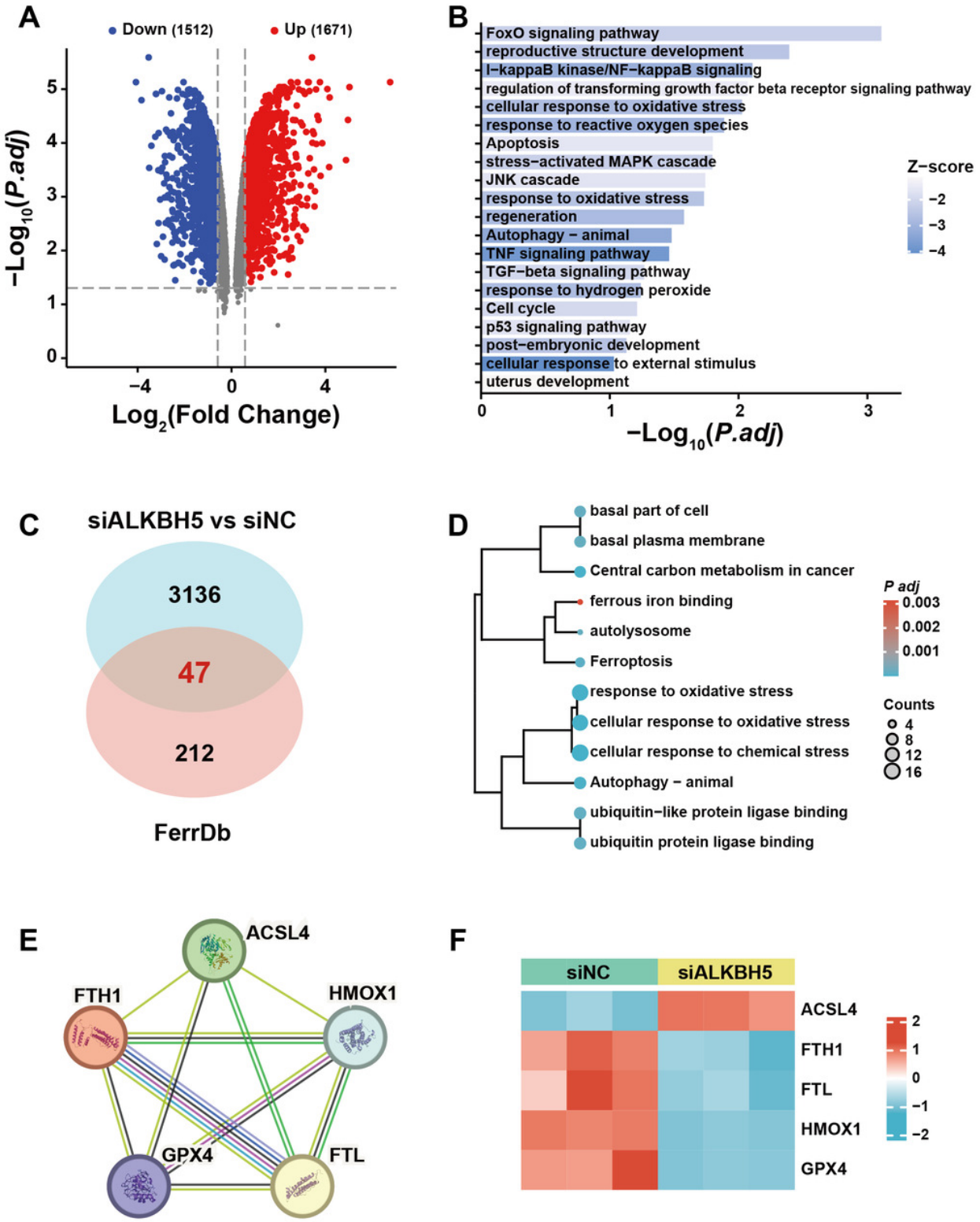
A
Down (1512)
Up (1671)
−Log10(P.adj)
Log2(Fold Change)
B
FoxO signaling pathway
reproductive structure development
I−kappaB kinase/NF−kappaB signaling
regulation of transforming growth factor beta receptor signaling pathway
cellular response to oxidative stress
response to reactive oxygen species
Apoptosis
stress−activated MAPK cascade
JNK cascade
response to oxidative stress
regeneration
Autophagy − animal
TNF signaling pathway
TGF−beta signaling pathway
response to hydrogen peroxide
Cell cycle
p53 signaling pathway
post−embryonic development
cellular response to external stimulus
uterus development
Z−score
−Log10(P.adj)
C
siALKBH5 vs siNC
3136
47
212
FerrDb
D
basal part of cell
basal plasma membrane
Central carbon metabolism in cancer
ferrous iron binding
autolysosome
Ferroptosis
response to oxidative stress
cellular response to oxidative stress
cellular response to chemical stress
Autophagy − animal
ubiquitin−like protein ligase binding
ubiquitin protein ligase binding
P adj
Counts
E
ACSL4
FTH1
HMOX1
GPX4
FTL
F
siNC
siALKBH5
ACSL4
FTH1
FTL
HMOX1
GPX4

Figure 6

ALKBH5 regulated the expression of FTL.

(A, B) Western blot showing that knockdown ALKBH5 reduced FTL protein levels. (C, D) Western blot showing that overexpression of ALKBH5 increased FTL protein levels. (E, F) Western blot showing that RSL3 increased the expression of FTL. (G, H) Western blot showing that FTL was increased in the villous tissues of patients with RM (n = 14) compared with that in HC (N = 14). (I, J, K) Representative immunohistochemical images depicting the expression of FTL in the villous tissues from patients with RM (n = 10) and HC (n = 10). (CTB, cytotrophoblast; STB, syncytiotrophoblast; *$p < 0.05$; **$p < 0.01$).

Figure 6

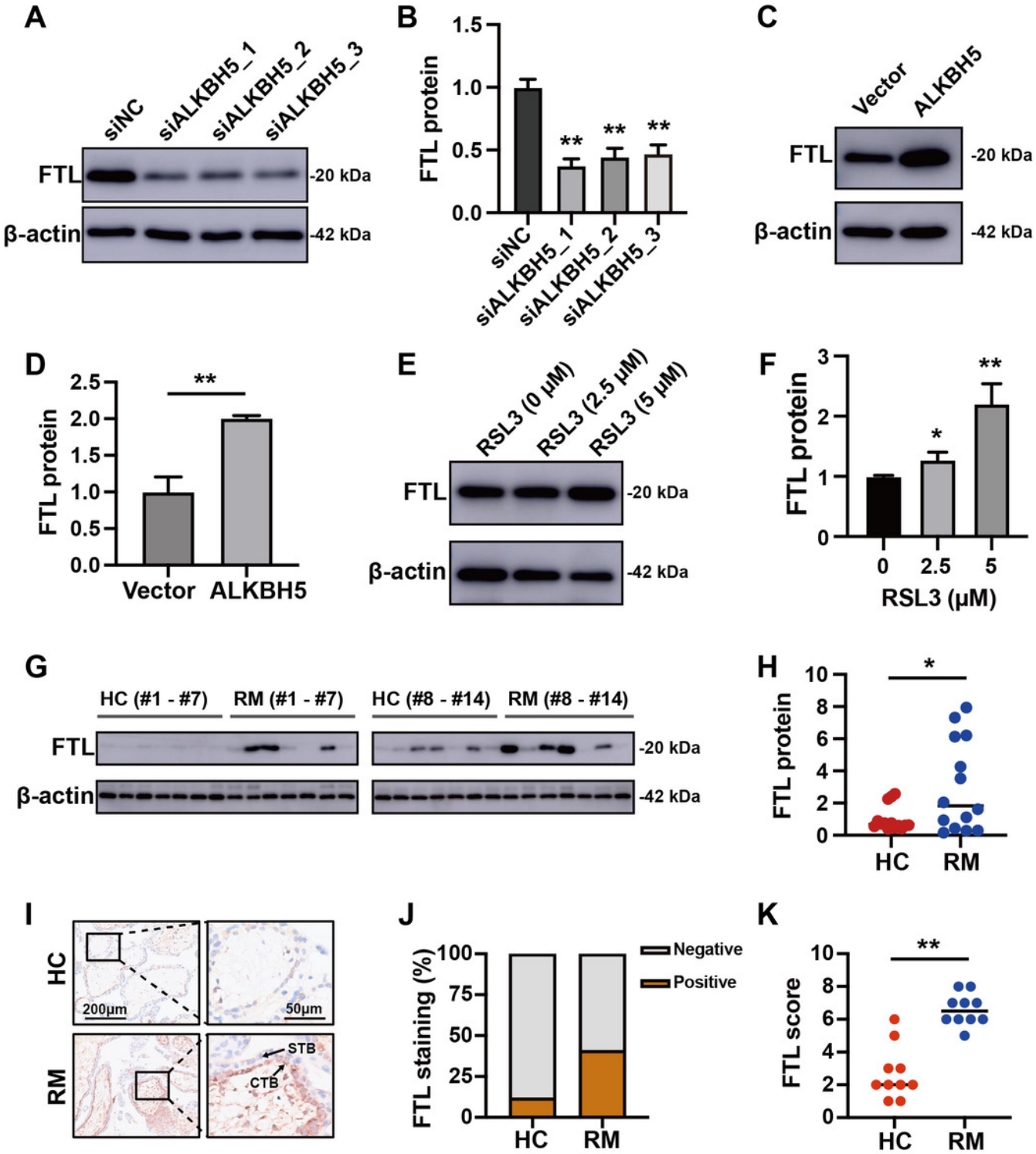
A
siNC
siALKBH5_1
siALKBH5_2
siALKBH5_3
FTL
β-actin
-20 kDa
-42 kDa
B
FTL protein
1.5
1.0
0.5
0.0
**
C
Vector
ALKBH5
D
2.5
2.0
1.5
1.0
0.5
0.0
Vector
ALKBH5
E
RSL3 (0 μM)
RSL3 (2.5 μM)
RSL3 (5 μM)
F
3
2
1
0
*
0
2.5
5
RSL3 (μM)
G
HC (#1 - #7)
RM (#1 - #7)
HC (#8 - #14)
RM (#8 - #14)
H
10
8
6
4
2
0
HC
RM
I
HC
RM
200μm
50μm
STB
CTB
J
FTL staining (%)
100
75
50
25
0
Negative
Positive
K
FTL score